

A Review on use of Infrared Thermography for Structural Condition Monitoring

Stephen M. Talai

Department of Mechanical and Production Engineering,
Moi University, Eldoret Kenya

Daniel K. Arusei, Lazarus K. Limo

Department of Mechanical and Production Engineering,
Moi University, Eldoret, Kenya

Abstract— Among the most common indicators of structural health of mechanical dynamic components are temperature and vibration levels. The online fault detection reduces the plant downtime, hence, increased availability and the overall efficiency. Infrared thermography (IRT) research has attracted a considerable attention in the recent. Therefore, this paper provides a review of the available approaches for condition monitoring of structural health. This will go a long way in providing recent research status as a dual condition monitoring tool for both temperature and vibration as indicators of health. This method has the ability of being employed in an inaccessible location or intention of additional proving of confidence of the existence of structural malfunctioning compared with the available techniques such as strain gauges which are tailored in monitoring only one indicator.

Keywords: *Damage detection, vibration analysis, online monitoring*

INTRODUCTION

In today's mechanical and aerospace engineering communities, need for enhanced ability to monitor dynamic structures and detect the potential damages at the earliest possible stage for effective structural health monitoring (SHM) is ever increasing [1]. Bagavathiappan et al. [2] reported that since the abnormal temperature pattern is an indication of the unhealthy state; it's widely used in temperature condition monitoring. The online temperature measurement performed in a non-contact way using Infrared thermography (IRT) aids early diagnosis of the probable faults and proper preventive measures adopted to avoid major shut downs.

The IRT based non-destructive testing and evaluation (NDT&E) techniques are among the most advanced techniques available today and have attracted much research attention [3-5]. Titman [6] explained that they represent the most promising method of structural defect detection using the principle that all bodies with an absolute temperature greater than 0 K emit infrared radiation. IRT can be classified into two major categories, namely; active and passive. **Error! Reference source not found.** depicts its schematic representation, including the related applications. Therefore, this paper first, provides the survey of active, secondly, passive IRT methods and finally, experimental methodologies for structural condition motoring.

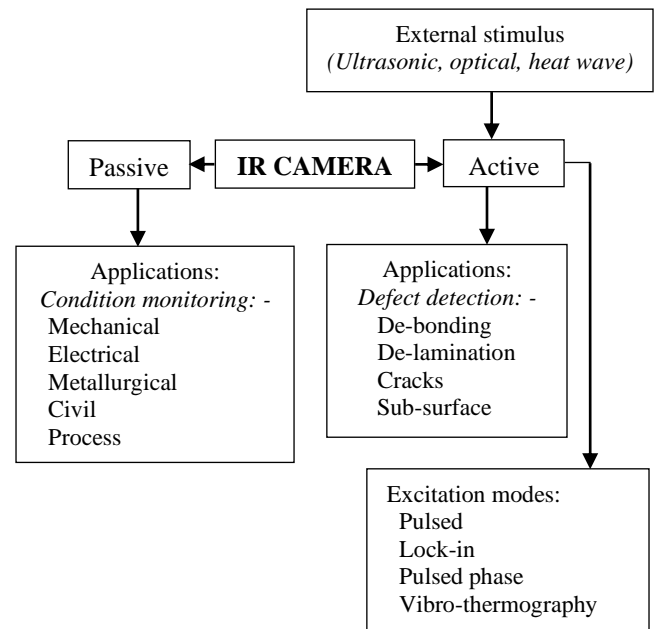


Figure 1. Classification of IRT and its applications [2].

ACTIVE INFRARED THERMOGRAPHY

The active IRT involves external stimulation of the structure to induce an internal heat flux [3], the structural condition will affect the heat diffusion and produce the corresponding thermal contrast on the surface being examined. The various methods of active IRT are described as follows:

Vibrothermography

Vibrothermography is a non-destructive evaluation technique used to discover surface and near surface defects such as cracks and delaminations through observations of vibration induced heat generation [7-10]. It involves exposing the specimen to a sonic or ultrasonic vibration, then observing the induced frictional heating with an infrared camera [11]. Mabrouki et al. [8] performed both numeral simulations and experimental studies using vibrothermography for detection of fatigue cracks in a steel compact tension specimen. The model revealed that the specimen's temperature increases at the crack vicinity according to the excitation frequency and is modulated due to non-linearity induced by the crack. The experimental results confirmed the potential of vibrothermography as a quick NDT&E method able to detect surface cracks.

Montanini and Freni [12] investigated the correlation between the vibrational mode shapes and viscoelastic heat generation in vibrothermography. The authors found that there exists a minimum threshold of vibrational amplitude

that allows for reliable flaw detections for specific geometries. The results indicated that exciting the specimen at its lower mode is sufficient to generate heat flux for identification of flaws.

Lahiri et al. [13] proposed an active IRT based technique for detecting defects in ferromagnetic specimens using low frequency alternating magnetic field induced heating. The results revealed a thermal contrast in the defective region that decays exponentially with the defect depth; therefore, the authors concluded that the proposed technique was suitable for rapid non-contact wide area inspection of ferromagnetic materials.

Lock-in thermography

The principle of lock-in thermography utilizes the application of a periodic input energy wave such as thermal emitter, ultrasound, microwave, eddy current or flash lamp to the surface of the object being examined, and thereafter analyzing the resulting local temperatures on the surface of the object [10, 14]. Palumbo et al. [10] investigated the use of lock-in thermography for de-bonding evaluation of composite adhesive joints. The approach proved an excellent NDT tool for evaluating the initial condition as a manufactured, bonded composite assembly, including being an effective tool to assess performance of parts under various environmental conditions. The authors concluded that the method has the ability to provide information regarding the suitability of the manufacturing process as well as an improvement in indicating bonding.

Pulsed thermography

The Pulsed thermography method utilizes infrared imaging of transient thermal patterns. It involves heating of the surface of the structure being tested using a high frequency pulse (of range 20 - 40 kHz) for a short time. The non-stationary heat distribution is then recorded during the entire period of the evolution [15, 16]. A "no defects" scenario in the specimen is associated with a uniform temperature rise. However, transient heat differs for zones with defects such as voids or delamination due to varying thermal parameters. The shape of the high-temperature zone represents the defect shape. Maldague [17] reported that the temperature distribution on the sample surface estimates the location, shape and size of the defect.

Pulsed phase thermography

Pulsed phase thermography combines pulsed thermography and phase/frequency concepts of the lock-in thermography [18, 19]. A modulated angular frequency emanating from a uniform source heats the specimen periodically while an IR camera remotely records the emerging thermal waves. Mezghani et al. [20] used pulsed thermography utilizing homogeneous heat provided by a laser source in the evaluation of paint thickness variations. The investigators analyzed thermal responses as a function of thermal properties and thickness of both coating and substrate layers. The results demonstrated that the thermal response of the paint coating is very well correlated to its thickness.

In general, the evaluation of composite material properties such as dis-bonding and crack detection has extensively utilized the pulsed phase thermography technique [21-24].

PASSIVE INFRARED THERMOGRAPHY

In passive thermography, no external heat is supplied to the object under examination. The object itself generates the stimulation heat for the IRT recording. Given that an abnormal temperature pattern is an indication of an unhealthy state, it is widely used in temperature condition monitoring [2]. The benefit of online temperature measurements performed in a non-contact fashion is that they aid in early diagnosis of the probable faults and proper preventive measures to be adopted to avoid major shutdowns.

Saidi et al. [25] reported that rotating machines bearing related faults are about 40% of the faults found most frequently, globally. Interestingly, Leemans et al. [26] successfully developed an auto-recursion model for on-line temperature measurement of rotating machine elements using IRT. This model detected drifts of less than one degree, thus, detecting the abnormal temperature evolution and prediction of potential failures. Singh et al. [27] carried out analysis of ball bearings under dynamic loading, using IRT and observed an increasing temperature trend for the bearing under an abrasion state.

Mazioud et al. [28] investigated the usage of IRT for detection of rolling bearing degradation and observed that a rise in temperature could be correlated with the level of vibration. Kim et al. [29] studied the fault diagnosis of ball bearings within rotational machines using the IRT method. The findings indicated that the method was well adapted for the monitoring and prognosis of bearing faults by qualitatively and quantitatively evaluating the temperature characteristics, according to the condition of the bearing.

Madruca et al. [30] used IRT for the real-time monitoring and control of the lead shield manufacturing process of a nuclear fuel and radioactive waste container. They observed that IRT represents an important tool to guarantee the proper homogeneity. Subsequently, studies indicate that IRT has been extensively applied to the total quality control through online monitoring of the fabrication process, including its subsequent assurance [31-39].

Moreover, IRT is amongst the most widely used tools for condition monitoring in the aerospace industry [2, 40]. Gao et al. [41] described the statistical method for finding an accurate vibrothermography inspection test procedure for the purpose of crack detection in aircraft engine fan blades. They showed that use of the Bayesian method enables the development of confidence intervals for the probability of detecting cracks. Meola et al. [42] used the lock-in thermography for monitoring damages such as delamination, impact and fatigue failure in various aerospace materials such as composites, hybrid composites and sandwich structures. They recommended that the use of IRT as a remote imaging system could be advantageous if incorporated in industrial instrumentation to control the entire manufacturing process and for quality assurance.

Furthermore, because the wind turbine blades are generally manufactured from composite materials, flaws and damage are inevitable during either their assembly or their operational lifetime. For this reason, IRT is used predominantly used for the diagnosis of premature failures and for increased reliability in both manufacturing quality control and in-

service inspection of structural integrity emanating from the defects [43-48].

Cardone et al. [49] used IRT to perform heat transfer measurements on a rotating disk in the laminar, transitional and turbulent flow regimes by making use of the heated-thin-foil technique and by measuring temperature gradients. They observed that the use of this technique was advantageous on account of its relatively good spatial resolution and thermal sensitivity and because it facilitates the recording of measurements down to very low local Reynolds numbers. Furthermore, Dimarogonas and Syrimbeis [50] successfully studied the thermal signature of a vibrating plate caused by material damping. They also indicated that an IRT based condition monitoring of mechanical equipment ensures the proper and healthy operation of plants, reduces downtime and maintenance cost and increases the plant's efficiency.

EXPERIMENTAL METHODOLOGIES FOR IRT BASED CONDITION MONITORING

A typical industrial application of IRT based condition monitoring on a dynamic mechanical component (*compressor motor*) including its thermal image is presented in **Figure 2**, where abnormal surface temperature in an indication of probable flaw.

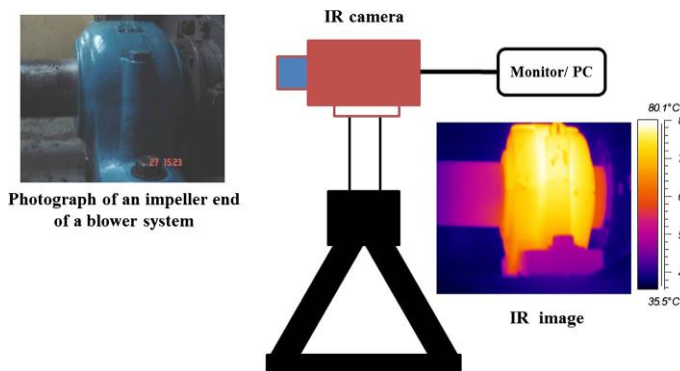


Figure 2. A typical practical setup for temperature based condition monitoring using IRT [2].

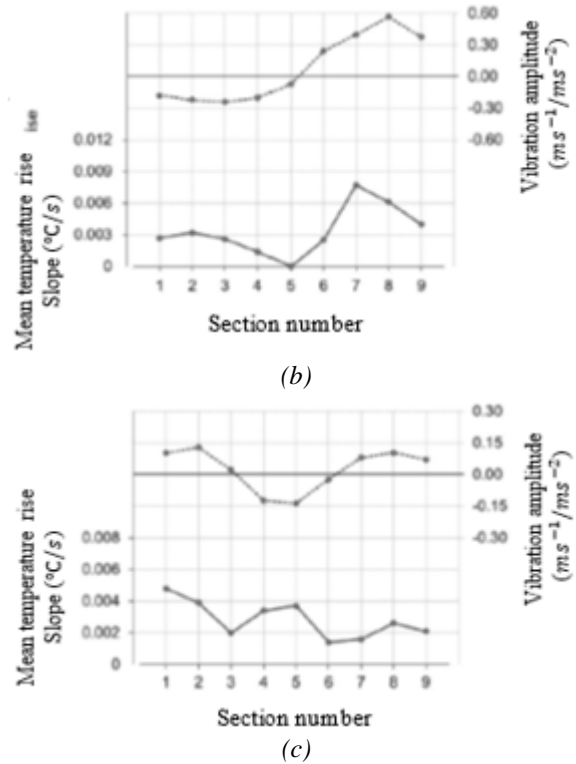
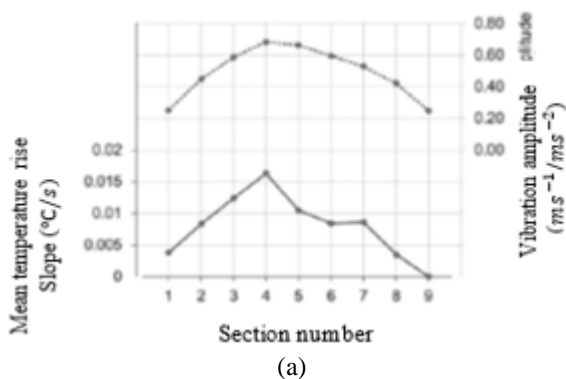


Figure 3. Vibration and heating profiles of defective beam vibrating at its resonance frequencies (a) first mode at mode at 15,944 Hz; (b) second mode at 16,418 Hz; (c) third mode at 17,471 Hz [53].

Accordingly, despite the large amount of research conducted on condition monitoring using IRT as indicated in the recent comprehensive literature review by Bagavathiappan et al. [2], little attention has been paid to vibration measurement. Interestingly, Dimarogonas and Syrimbeis [50] successfully studied the vibration modes from thermal signature of a vibrating plate due to material damping. From the elasticity theory, there exists a strong relationship between vibration and temperature signature. Dimarogonas et al. [51] positively quantified the heating effect for rotating shafts and reported substantial temperatures development during lateral and torsional vibration due to heat transients, causing s in the elastic and plastic deformation range. Harrison [52] utilized temperature distribution of a pump coupler to confirm existence of its vibration, thus; concluded that probably where there's heat increase in a dynamic component, probably there's vibration. Montanini and Freni [12] used rectangular AISI 304 steel beam to study the correlation between vibrational mode shapes and viscoelastic heat generation in vibrothermography. The beam was excited at its first three resonance frequencies. Their findings are presented in Error! Reference source not found.. Mazioud et al. [28] studied the existing relationship of vibration with temperature increase on detection of rolling bearing degradation using infrared thermography. The authors' inferred that temperature increases with increase in vibration magnitudes (Figure 4).

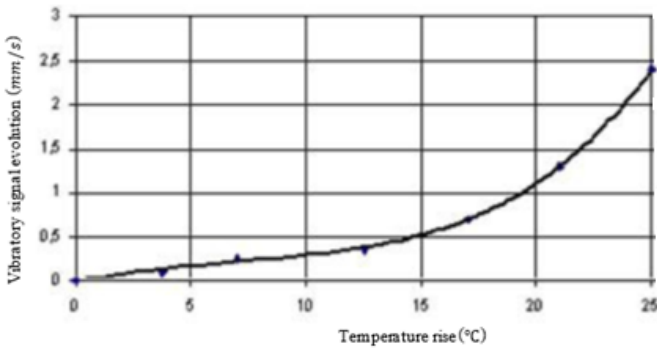


Figure 4. Evolution of the temperature of the bearing cap according to the vibratory level [28].

It is known that the presence of crack or contact interface in a vibrating structure will act as a friction interface, thus, a heat

source generation since it forms a sink for dissipation of vibratory energy [54]. However, Singh and Lucas [55] reported that the phenomenon of predicting of structural vibration characteristics from thermal generation is not well understood, hence, many researchers are actively working towards understanding it.

Talai et al. [56] studied the vibration characteristics measurement of beam-like structures using infrared thermography. They considered a suitable manufactured rig, fixed the beams and friction rod as required. The laboratory experimental setup was as presented in Figure 5. Two infrared cameras were used. The Micro-epsilon TIM160 infrared camera focused on the friction interface of beam 1.

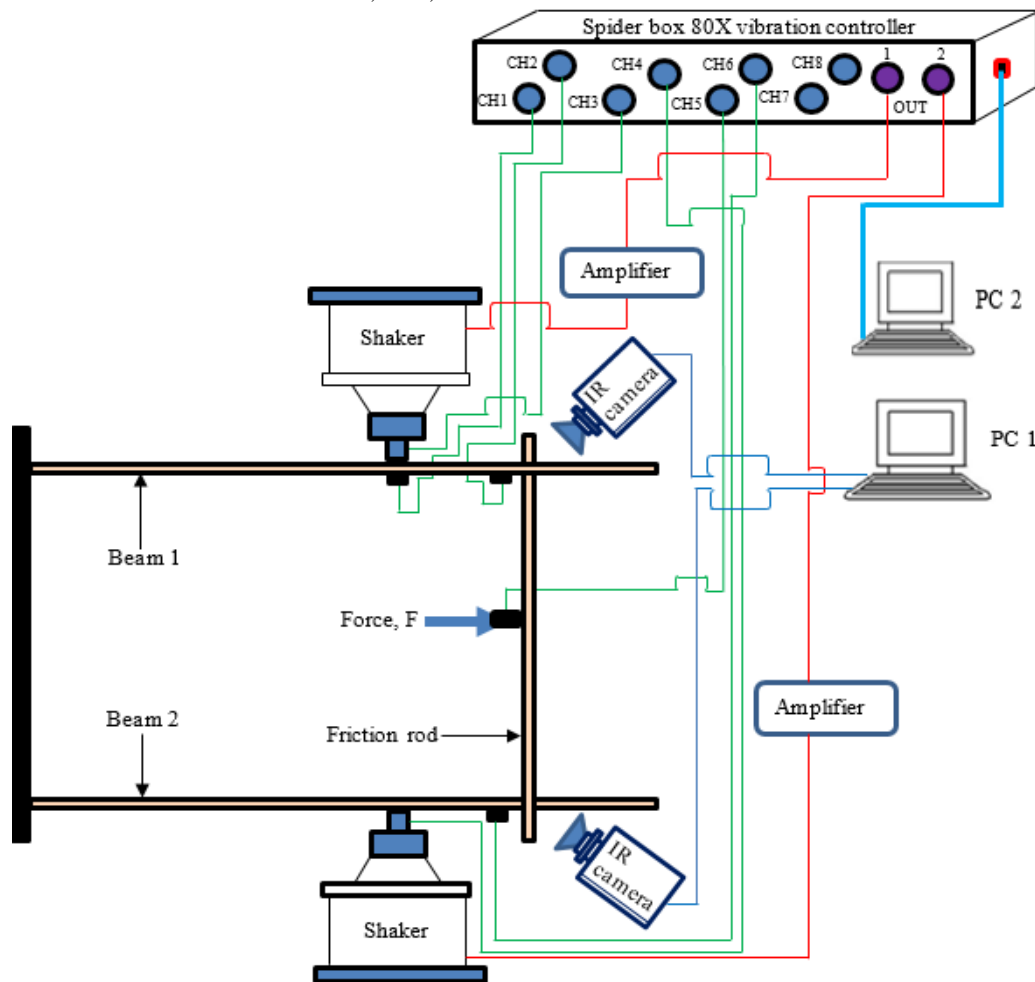


Figure 5. Laboratory experimental setup [56].

Its properties includes: thermal sensitivity of 80 mK, spectral range of 7.5 - 13 μm, optical resolution of 160 × 120 Pixels, frame rate real time of 120 Hz and lenses FOV of 23 °. On the hand, Flir A325sc infrared camera focused on the friction interface of beam 2. Its properties includes: thermal sensitivity of 50 mK, spectral range of 7.5 -13μm, optical resolution of 320 × 240 Pixels, frame rate real time of 60 Hz and lenses FOV of 25 °. Spider box X80 vibration controller (operated by PC 2) firstly, generated the required signals through the output 1 and 2 for vibration shaker attached to

beam 1 (Brüel & Kjør, model 4824) and beam 2 (Sentek, model MS-1000), respectively. The signal for the former was amplified by Brüel & Kjør, model 2732 amplifier while the latter by Sentek, model LA 1500 amplifier. These facilitated the beams mechanical excitation. Secondly, controlled the vibration excitation via channel 1 by a miniature Deltatron accelerometer type 4507 (sensitivity of 9.989 mV/ms⁻²) attached to beam 1 for closed loop operation, thus, protecting the shakers against the sudden overloads. Thirdly, recorded the beam dynamic responses through channel 2 and 6 via

miniature Deltatron accelerometers type 4507 (sensitivity of 1.025 mV/ms^{-2}) attached to beam 1 and 2, respectively (attached at 2 mm from the interface and opposite side of the zone under focus by an IR camera to avoid interference of thermal recording). The aim of this was for validation of vibration parameters predicted using IRT approach. The two sets of experiments were carried out. First, exciting both beams at 20 Hz. Secondly, exciting beam 1 at 40 Hz and beam 2 at 20 Hz. The excitation frequencies were considered based on the sampling rule of 2.5 times the sampling rate in relation to the rated optical resolution of the IR cameras. For the entire excitation period, the thermal images were recorded continuously for 150 s and the images stored in the PC 1 for post analysis.

The time-domain temperature wave forms were analysed using a MATLAB algorithm. Therefore, the vibration frequencies evaluated for Beam 1 and Beam 2 were 19.9885 Hz (Figure 6a) and 19.9973 Hz (Figure 6b), respectively. These were in good agreement with those measured using the accelerometer with the relative difference being 0.26 % and 0.21 % for the former and latter, respectively. The several smaller frequency peaks observed with Beam 1 were associated to the beam multi-dynamics due to periodic loading.

In the case of 40 Hz and 20 Hz beam excitation for Beam 1 and Beam 2, respectively; the analyzed frequencies were 39.9686 Hz (Figure 7a) and 20.000 Hz (Figure 7b) for Beam 1 and Beam 2, respectively. Compared to the accelerometer measured frequencies, relative difference was 0.28 % and 0.20 % for the former and latter, respectively.

Similar findings were obtained Talai et al. [57] in their work of comparison of infrared thermography and miniature Deltatron accelerometer sensors in the measurement of structural vibration characteristics found that frictional temperature signature predicts the structural vibration frequency just as obtained from displacement.

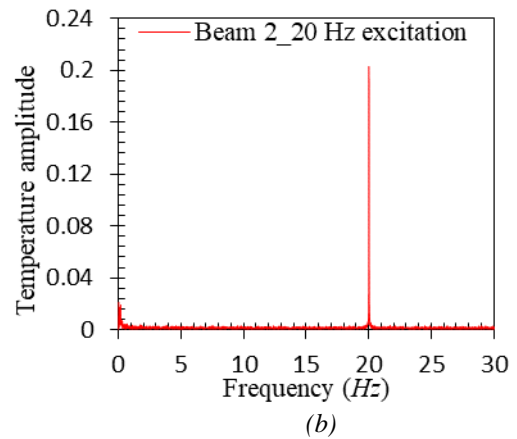
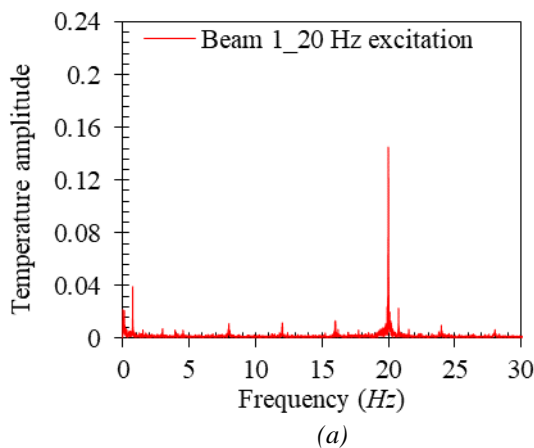


Figure 6. FFT of temperature evolution for both beams excited at 20 Hz (a) Beam 1 & (b) Beam 2

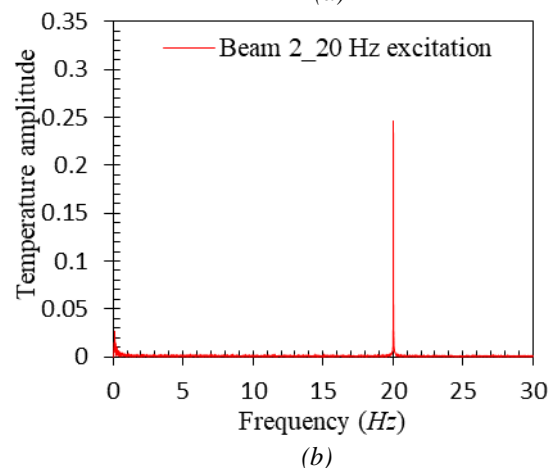
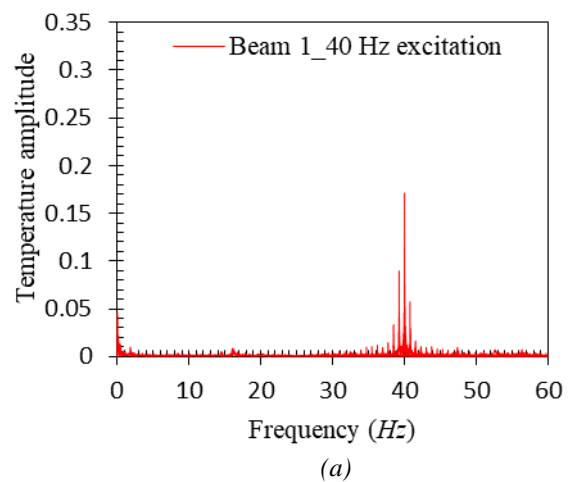


Figure 7. FFT of temperature evolution (a) Beam 1 at 40 Hz & (b) Beam 2 at 20 Hz

Further, Talai et al. [58] numerically studied the prediction of structural vibration frequency from frictional heat generation. The model assembly was as shown in **Error! Reference source not found.** For the purpose of simulating the structural mechanical excitations of the laced beams, the sinusoidal loads were defined on the beams' surface while a lateral force to the lacing wire. The forced excitations were achieved through the formulation of a sinusoidal load using a varying force function.

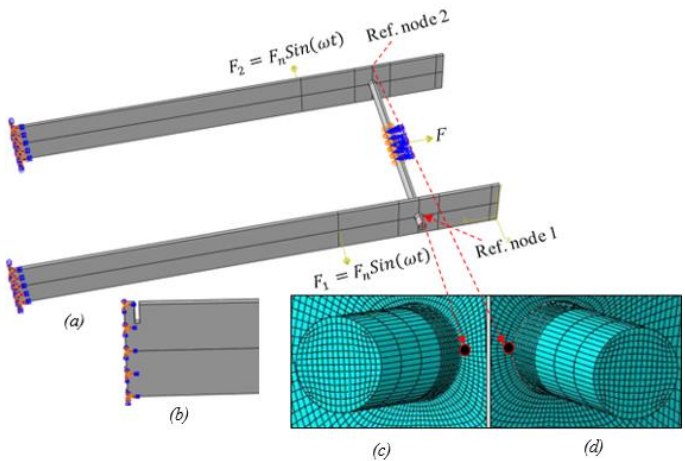


Figure 8. FEM model (a) assembly, boundary conditions and loading (b) beam 1 induced with defect-1mm wide and 5 mm deep (c) beam 1 interface mesh with a reference node (d) beam 2 interface mesh with a reference node [58].

Primarily, it is known that frictional heating concentrates within the real area of contact between two bodies in relative motion. Montanini and Freni [12] explained that the amount of frictional heat generated depends on several parameters, which includes coefficient of friction, normal applied force and the sliding relative speed. However, this study kept other factors constant while the forcing frequencies (relative speed) varied. Also, Mabrouki et al. [8] reported that frictional energy consumed or stored in the material as micro-structural changes such as dislocations and phase transformation in general is about 5%. The remaining part of the friction energy raises the interface temperature. Furthermore, according to the coulomb law of friction, frictional heat generation occurs only if there exists a relative motion between the interacting structures [59]. This means that the frictional temperature signature is consistent with the displacement pattern, as evidenced by displacement and frictional temperature time domain waveform for the simulation of both beams excited at 40 Hz (Error! Reference source not found.). As expected, the structure under higher excitation frequency allows the frictional interface to slide against each other more times; unlike at lower frequencies, hence, leading to greater frictional temperature evolution. This is supported by the work of Mabrouki et al. [8] who observed similar findings on investigation of the frictional heating model for efficient use of vibrothermography. Hence, the conclusion was that frictional heat increases with the interface frequency. The analysed frequencies are presented Figure 9b. The extracted frequency from frictional temperature signature was 39.99 Hz. This was in good agreement with that acquired from the corresponding displacement as 39.99 Hz.

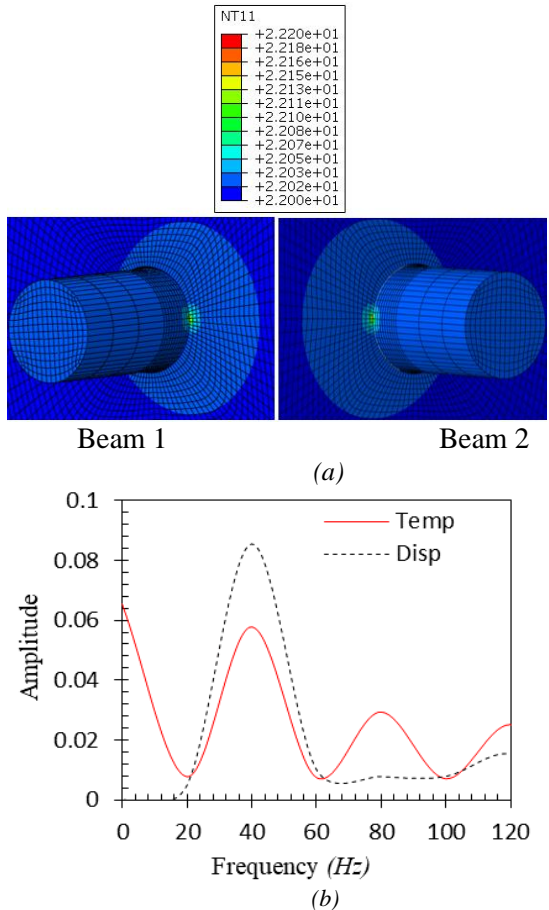
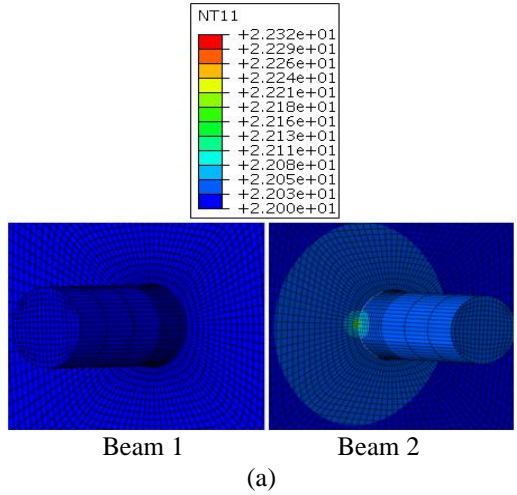


Figure 9. Both beams excited at 40 Hz (a) interface temperature contour (b) FFT of temperature evolution and displacement.

In the case of beams excitation at different forcing frequencies of beam 1 at 20 Hz and beam 2 at 40 Hz; the results revealed a frictional temperature increase of 0.24 and 0.32 °C in the former and latter, respectively (Figure 10a). Authors found that frictional temperature evolution incredibly predicted the vibration frequency just like displacement curves (Figure 10b) as shown in Error! Reference source not found..



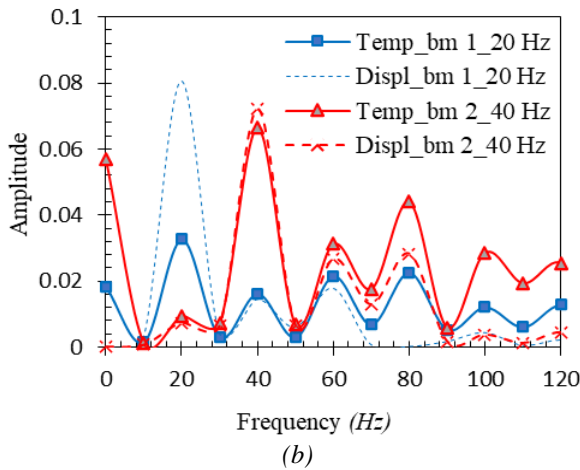


Figure 10. Beam 1 excited at 20 Hz and beam 2 at 40 Hz (a) interface temperature contour (b) FFT of temperature evolution and displacement [58].

Table 1. FEA frequencies with different excitation frequencies.

Forcing frequency	Results	Frequency predicted	
		Temp. signature	Disp. curve
Beam 1: 20 Hz	Figure 8b	19.99 Hz	19.99 Hz
Beam 2: 40 Hz		39.97 Hz	39.97 Hz

Also, they found the values to agree well with those corresponding to the forcing frequency. This implies that the irrespective of the structural excitations, the analysis of the interface frictional heat evolution is capable enough of predicting its vibration frequency as evidenced by these findings.

The crack existence reduces the stiffness of a structural member due to local flexibility. Dimarogonas [60], analytically examined the forced vibration of a cracked cantilever beam. The author found that dynamic deflection increases due to crack. As a result, this increases the frictional temperature evolution as shown by the similar contour interface temperature for the healthy model (Figure 11a) and vice versa for a model with induced defect (Figure 11b).

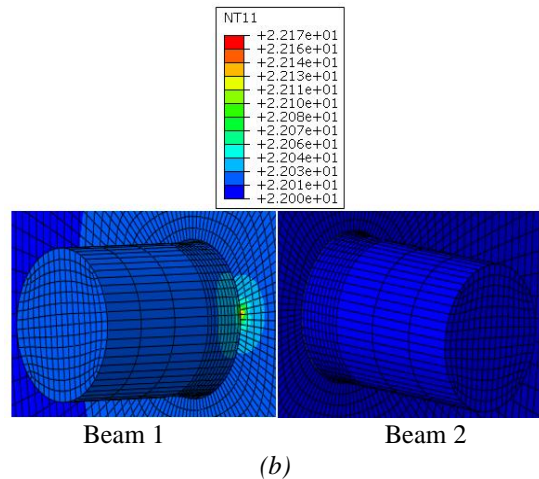
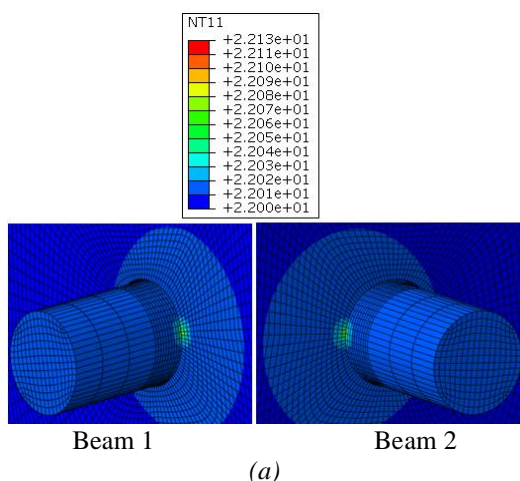


Figure 11. Interface temperature contour for both beams excited at 25 Hz after 0.08 s (a) Both beams are healthy (b) Beam 1 induced with defect while beam 2 is healthy.

Even though the frequencies analyzed from the frictional temperature signatures and displacements were in good agreement in both models as 25.00 Hz (Error! Reference source not found.), the authors observed a significant variation in peaks.

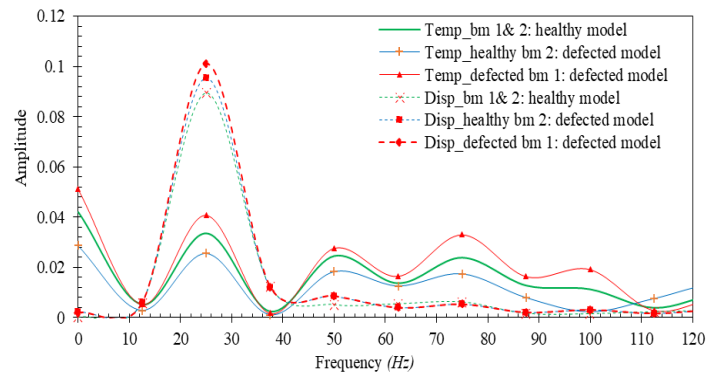


Figure 12. FFT of temperature evolution and displacement for both healthy & defected FE beam models [58].

Hence, considering the model with an induced defect in comparison to the healthy model as a reference; peak for thermally acquired frequency in the case of beam induced with a defect increased and vice versa for the healthy while both increased in the case of displacements. This shows that presence of structural defect alters the frequency peaks, however, the predominant frequency will be identified based on the spectral peak.

CONCLUSION

Machinery structural failures particularly arising from vibration related phenomenon remains the major frequent cause of downtime. The suitability for structural vibration monitoring technique is critical in maintaining its integrity. This literature review, clearly it shows that there is a need for the quantification of thermal heat emanating from structural vibration providing online condition monitoring with two indicators (vibration and thermal signature) using a single

customized tool. This will be a major milestone for a strong and reliable approach for maintaining structural integrity.

ACKNOWLEDGEMENT

The author greatly appreciates the support of Moi university, Kenya and Tshwane University of Technology, Republic of South Africa.

REFERENCES

- [1] Le, TTH, Point N, Argoul P, Cumunel G. Structural changes assessment in axial stressed beams through frequencies variation. *International Journal of Mechanical Sciences* 2016; 110: 41-52.
- [2] Bagavathiappan, S, Lahiri BB, Saravanan T, Philip J, Jayakumar T. Infrared thermography for condition monitoring – A review. *Infrared Physics & Technology* 2013; 60: 35-55.
- [3] Gong, J, Liu J, Wang F, Wang Y. Inverse heat transfer approach for nondestructive estimation the size and depth of subsurface defects of CFRP composite using lock-in thermography. *Infrared Physics & Technology* 2015; 71: 439-447.
- [4] Meola, C, Carlomagno GM, Giorleo L. The use of infrared thermography for materials characterization. *Journal of Materials Processing Technology* 2004; 155(156): 1132-1137.
- [5] Aldave, JI, Bosom VP, González LV, López de Santiago I, Vollheim B, Krausz L, Georges M. Review of thermal imaging systems in composite defect detection. *Infrared Physics & Technology* 2013; 61: 167-175.
- [6] Titman, DJ. Applications of thermography in non-destructive testing of structures. *NDT&E International* 2001; 34: 149-154.
- [7] Renshaw, J, Chen JC, Holland SD, Bruce TR. The sources of heat generation in vibrothermography. *NDT&E International* 2011; 44(8): 736-739.
- [8] Mabrouki, F, Thomas M, Genest M, Fahr A. Frictional heating model for efficient use of vibrothermography. *NDT&E International* 2009; 42(5): 345-352.
- [9] Rizi, AS, Hedayatrasa S, Maldague X, Vukhanh T. FEM modeling of ultrasonic vibrothermography of a damaged plate and qualitative study of heating mechanisms. *Infrared Physics & Technology* 2013; 61: 101-110.
- [10] Palumbo, D, Tamborrino R, Galietti U, Aversa P, Tati A, Luprano VAM. Ultrasonic analysis and lock-in thermography for debonding evaluation of composite adhesive joints. *NDT&E International* 2016; 78: 1-9.
- [11] Holland, SD, Uhl C, Ouyang Z, Bantel T, Li M, Meeker WQ, Lively J, Brasche L, Eisenmann D. Quantifying the vibrothermographic effect. *NDT&E International* 2011; 44(8): 775-782.
- [12] Montanini, R, Freni F. Correlation between vibrational mode shapes and viscoelastic heat generation in vibrothermography. *NDT&E International* 2013; 58: 43-48.
- [13] Lahiri, BB, Bagavathiappan S, C. Soumya C, Mahendran V, Pillai VPM, J. JP, Jayakumar T. Infrared thermography based defect detection in ferromagnetic specimens using a low frequency alternating magnetic field. *Infrared Physics & Technology* 2014; 64: 125-133.
- [14] Zhang, J-Y, Meng X-b, Ma Y-c. A new measurement method of coatings thickness based on lock-in thermography. *Infrared Physics & Technology* 2016; 76: 655-660.
- [15] Montanini, R, Freni F. Investigation of heat generation sources in sonic infrared thermography using laser Doppler vibrometry. *In: 11th International Conference on Quantitative InfraRed Thermography*. Italy: Naples 2012.
- [16] Tang, Q, Dai J, Liu J, Liu C, Liu Y, Ren C. Quantitative detection of defects based on Markov-PCA-BP algorithm using pulsed infrared thermography technology. *Infrared Physics & Technology* 2016; 77: 144-148.
- [17] Maldague, X, *Theory and practice of infrared technology for nondestructive testing*. 2001: Wiley.
- [18] Maldague, X, Galmiche F, Ziadi A. Advances in pulsed phase thermography. *Infrared Physics & Technology* 2002; 43: 172-181.
- [19] Ibarra-Castanedo, C, González D, Klein M, Pilla M, Vallerand S, Maldague X. Infrared image processing and data analysis. *Infrared Physics & Technology* 2004; 46(1-2): 75-83.
- [20] Mezghani, S, Perrin E, Vrabie V, Bodnar JL, Marthe J, Cauwe B. Evaluation of paint coating thickness variations based on pulsed Infrared thermography laser technique. *Infrared Physics & Technology* 2016; 76: 393-401.
- [21] Waugh, RC, Dulieu-Barton JM, Quinn S. Modelling and evaluation of pulsed and pulse phase thermography through application of composite and metallic case studies. *NDT&E International* 2014; 66: 52-66.
- [22] Shin, PH, Webb SC, Peters KJ. Pulsed phase thermography imaging of fatigue-loaded composite adhesively bonded joints. *NDT&E International* 2016; 79: 7-16.
- [23] Gao, Y, Tian GY, Li K, Ji J, Wang P, Wang H. Multiple cracks detection and visualization using magnetic flux leakage and eddy current pulsed thermography. *Sensors and Actuators A: Physical* 2015; 234: 269-281.
- [24] Chang, Y-S, Yan Z, Wang K-H, Yao Y. Non-destructive testing of CFRP using pulsed thermography and multi-dimensional ensemble empirical mode decomposition. *Journal of the Taiwan Institute of Chemical Engineers* 2016; 61: 54-63.
- [25] Saidi, L, Ali JB, Benbouzid M, Bechhoefer E. The use of SESK as a trend parameter for localized bearing fault diagnosis in induction machines. *ISA Transactions* 2016; 63: 436-447.
- [26] Leemans, V, Destain M, Kilundu B, Dehombreux P. Evaluation of the Performance of Infrared Thermography for On-Line Condition Monitoring of Rotating Machines. *Engineering* 2011; 3(10): 1030-1039.
- [27] Singh, RC, Pandey RK, Chaudhary R, S. RM, Saxena H. Analysis of Ball Bearings under Dynamic Loading Using Non-Destructive Technique of Thermography. *International Journal of Advance Research and Innovation* 2014; 2(4): 781-783.
- [28] Mazioud, A, Ibos L, Khlaifi A, Durastanti JF. Detection of rolling bearing degradation using infrared thermography. *In: 9th International Conference on Quantitative InfraRed Thermography*. Poland: Krakow 2008.
- [29] Kim, DS, Yun H, Yang S, Kim W, Hong D. Fault diagnosis of ball bearing within rotational machines using infrared thermography method. *Journal of the Korean Society for Nondestructive Testing* 2010; 30(6): 558-563.
- [30] Madruga, FJ, González DA, Mirapeix JM, López Higuera JM. Application of infrared thermography to the fabrication process of nuclear fuel containers. *NDT&E International* 2005; 38(5): 397-401.
- [31] Lee, S, Namb J, W. H, Kimb J, Lee B. A study on integrity assessment of the resistance spot weld by Infrared Thermography. *Procedia Engineering* 2011; 10: 1748-1753.
- [32] Alfaro, SCA, Vargas JAR, de Carvalho GC, de Souza GG. Characterization of “Humping” in the GTA welding process using infrared images. *Journal of Materials Processing Technology* 2015; 223: 216-224.
- [33] Mattei, S, Grevey D, Mathieu A, Kirchner L. Using infrared thermography in order to compare laser and hybrid (laser+MIG) welding processes. *Optics & Laser Technology* 2009; 41(6): 665-670.
- [34] Mirapeix, J, Vila E, Valdiande JJ, Riquelme A, Garcia M, Cobo A. Real-time detection of the aluminium contribution during laser welding of Usibor1500 tailor-welded blanks. *Journal of Materials Processing Technology* 2016; 235: 106-113.
- [35] Rodríguez-Martin, M, Lagüela S, González-Aguilera D, Arias P. Cooling analysis of welded materials for crack detection using infrared thermography. *Infrared Physics & Technology* 2014; 67: 547-554.
- [36] Rodríguez-Martín, M, Lagüela S, González-Aguilera D, Martínez J. Thermographic test for the geometric characterization of cracks in welding using IR image rectification. *Automation in Construction* 2016; 61: 58-65.
- [37] Saravanan, T, Lahiri BB, Arunmuthu K, Bagavathiappan S, Sekhar AS, Pillai VPM, Philip J, Rao BPC, Jayakumar T. Non-destructive Evaluation of Friction Stir Welded Joints by X-ray Radiography and Infrared Thermography. *Procedia Engineering* 2014; 86: 469-475.
- [38] Speka, M, Mattei S, Pilloz M, Ilie M. The infrared thermography control of the laser welding of amorphous polymers. *NDT&E International* 2008; 41(3): 178-183.
- [39] Degidi, M, Nardi D, Sighinolfi G, Merla A, Piattelli A. In vitro infrared thermography assessment of temperature peaks during

- the intra-oral welding of titanium abutments. *Infrared Physics & Technology* 2012; 55(4): 279-283.
- [40] Meola, C, Carlomagno GM. Recent advances in the use of infrared thermography. *Measurement Science and Technology* 2004; 15(9): 27-58.
- [41] Gao, C, Meeker WQ, Mayton D. Detecting cracks in aircraft engine fan blades using vibrothermography nondestructive evaluation. *Reliability Engineering and System Safety* 2014; 131: 229-235.
- [42] Meola, C, Carlomagno GM, Squillace A, Vitiello A. Non-destructive evaluation of aerospace materials with lock-in thermography. *Engineering Failure Analysis* 2006; 13(3): 380-388.
- [43] Avdelidis, NP, Gan TH. *Non-destructive evaluation (NDE) of Composites: infrared (IR) thermography of wind turbine blades*, in *Non-Destructive Evaluation (NDE) of Polymer Matrix Composites*. 2013, Woodhead Publishing. p. 634-650.
- [44] Beganovic, N, Söffker D. Structural health management utilization for lifetime prognosis and advanced control strategy deployment of wind turbines: An overview and outlook concerning actual methods, tools, and obtained results. *Renewable and Sustainable Energy Reviews* 2016; 64: 68-83.
- [45] Martinez-Luengo, M, Kolios A, Wang L. Structural health monitoring of offshore wind turbines: A review through the Statistical Pattern Recognition Paradigm. *Renewable and Sustainable Energy Reviews* 2016; 64: 91-105.
- [46] Schubel, PJ, Crossley RJ, Boateng EKG, Hutchinson JR. Review of structural health and cure monitoring techniques for large wind turbine blades. *Renewable Energy* 2013; 51: 113-123.
- [47] Worzewski, T, Krankenhagen R, Doroshtnasir M, Röllig M, Maierhofer C, Steinfurth H. Thermographic inspection of a wind turbine rotor blade segment utilizing natural conditions as excitation source, Part I: Solar excitation for detecting deep structures in GFRP. *Infrared Physics & Technology* 2016; 76: 756-766.
- [48] Yang, R, He Y, Zhang H. Progress and trends in non-destructive testing and evaluation for wind turbine composite blade. *Renewable and Sustainable Energy Reviews* 2016; 60: 1225-1250.
- [49] Cardone, G, Astarita T, Carlomagno GM. Heat transfer measurements on a rotating disk. *Int: International Journal of rotating machinery* 1997; 3(1): 1-9.
- [50] Dimarogonas, AD, Syrimbeis NB. Thermal signatures of vibrating rectangular plates. *Journal of Sound and Vibration* 1992; 157(3): 467-476.
- [51] Dimarogonas, AD, Paipetis SA, Chondros TG. *Analytical Methods in Rotor Dynamics* (second edition) New York London: Springer Dordrecht Heidelberg: 2013: 203-263.
- [52] Harrison, LR. Shake, Rattle & Roll: Where's there's Heat There's Probably Vibration. *Sound and vibration* 2003; 37(5): 8-9.
- [53] Montanini, R, Freni F. Correlation between vibrational mode shapes and viscoelastic heat generation in vibrothermography. *NDT & E International* 2013; 58: 43-48.
- [54] Rao, SJ. *Turbo-machine blade vibration* (first edition). New Delhi: New age international publishers 1991: 7-20.
- [55] Singh, M, Lucas G. *Blade design & analysis for steam turbines*. The McGraw-Hill Companies: United States of America 2011: 20-60.
- [56] Talai, SM, Desai DA, Heyns PS. Vibration characteristics measurement of beam-like structures using infrared thermography. *Infrared Physics & Technology* 2016; 79: 17-24.
- [57] Talai, SM, Desai DA, Heyns PS. Comparison of infrared thermography and miniature Deltatron accelerometer sensors in the measurement of structural vibration characteristics. *African Journal of Science, Technology, Innovation and Development* 2017.
- [58] Talai, SM, Desai DA, Heyns PS. Experimentally validated structural vibration frequencies' prediction from frictional temperature signatures using numerical simulation: A case of laced cantilever beam-like structures. *Advances in Mechanical Engineering* 2017; 9(1): 1-10.
- [59] Simar, A, Bréchet Y, de Meester B, Denquin A, Gallais A, Pardoën T. Integrated modeling of friction stir welding of 6xxx series Al alloys Process, microstructure and properties. *Progress in Materials Science* 2012; 57: 95-187.
- [60] Dimarogonas, AD. Vibration of cracked structures: A state of the art review. *Engineering Fracture Mechanics* 1996; 55(5): 831-857.